Lecture Notes in Civil Engineering

Edmund Lorencowicz
Bruno Huyghebaert
Jacek Uziak *Editors*

Farm Machinery and Processes Management in Sustainable Agriculture

XII International Scientific Symposium 2024

Springer

Edmund Lorencowicz · Bruno Huyghebaert ·
Jacek Uziak
Editors

Farm Machinery and Processes Management in Sustainable Agriculture

XII International Scientific Symposium 2024

Springer

Editors
Edmund Lorencowicz
Faculty of Production Engineering
University of Life Sciences
Lublin, Poland

Bruno Huyghebaert
Walloon Agricultural Research Centre
Gembloux, Belgium

Jacek Uziak
College of Management and Enterprise
Wałbrzych, Poland

ISSN 2366-2557 ISSN 2366-2565 (electronic)
Lecture Notes in Civil Engineering
ISBN 978-3-031-70954-8 ISBN 978-3-031-70955-5 (eBook)
https://doi.org/10.1007/978-3-031-70955-5

This Springer imprint is published by the registered company Springer Nature Switzerland AG
The registered company address is: Gewerbestrasse 11, 6330 Cham, Switzerland

Organization

Scientific Committee

Chairmen

Edmund Lorencowicz	University of Life Sciences in Lublin, Poland
Bruno Huyghebaert	CRA-W Gembloux, Belgium

Members

Alex Folami Adisa	Federal University of Agriculture, Abeokuta, Nigeria
Arlindo Almeida	Polytechnic Institute of Bragança, Portugal
Atanas Zdravkov Atanasov	"Angel Kanchev" University of Ruse, Bulgaria
Fatima Baptista	University of Évora & MED– Mediterranean Institute for Agriculture, Environment and Development, Portugal
Volodymyr Bulgakov	University of Life and Environmental Sciences of Ukraine, Kyiv, Ukraine
Philippe Burny	Walloon Agricultural Research Centre & Gembloux Agro-Bio Tech, University of Liege, Gembloux, Belgium
Karl-Heinz Dammer	ATB Leibnitz-Institut für Agrartechnik und Bioökonomie, Potsdam, Germany
Ester Foppa Pedretti	Marche Polytechnic University, Ancona, Italy
Fran Gjoka	Agricultural University of Tirana, Albania
Sławomir Kocira	University of Life Sciences in Lublin/Poland & University of South Bohemia in České Budějovice, Czechia
Milan Koszel	University of Life Sciences in Lublin, Poland
Artur Kraszkiewicz	University of Life Sciences in Lublin, Poland
José Rafael Marques da Silva	University of Évora, Portugal
Radko Mihaylov	Technical University of Varna, Bulgaria
Paula A. Misiewicz	Harper Adams University, UK
Gerhard Moitzi	BOKU-University of Natural Resources and Life Sciences, Vienna, Austria
Janusz Nowak	University of Life Sciences in Lublin, Poland

Jüri Olt	Estonian University of Life Sciences, Tartu, Estonia
Taskin Oztas	Atatürk University, Erzurum, Turkey
Athanassios Papageorgiou	Technological Educational Institute of Peloponnese, Kalamata, Greece
Stanisław Parafiniuk	University of Life Sciences in Lublin, Poland
Simone Pascuzzi	University of Bari Aldo Moro, Italy
Fabienne Rabier	CRA-W Gembloux, Belgium
Francesco Santoro	University of Bari Aldo Moro, Italy
Giacomo Scarascia-Mugnozza	Polytechnic of Bari, Italy
Yves Schenkel	CRA-W Gembloux, Belgium
Enkeleda Shkurta	National Environmental Agency & Polytechnic University of Tirana, Albania
Alaa Subr	College of Agricultural Engineering Sciences, University of Baghdad, Iraq
Hop Tho Hi Min	Gembloux Agro-Bio Tech, University of Liege, Belgium
Jacek Uziak	College of Management and Enterprise, Wałbrzych, Poland
Viktor Vojnich	University of Szeged, Hungary
Jens Karl Wegener	JKI Institute for Application Techniques in Plant Protection, Braunschweig, Germany

Contents

Theory of Operation of a Safety Finger Coupling Applied in the Drive of a Screw Conveyor for Bulk Agricultural Materials

Volodymyr Bulgakov[1], Simone Pascuzzi[2(✉)], Jüri Olt[3], Arlindo Almeida[4], Oleksandra Trokhaniak[1], Janusz Nowak[5], Yevhen Ihnatiev[3,6], Zbigniew Kiernicki[7], Francesco Paciolla[8,9], and Giacomo Scarascia Mugnozza[9]

[1] Department of Mechanics, National University of Life and Environmental Sciences of Ukraine, 15 Heroiv Oborony Str., Kyiv 03041, Ukraine

[2] Department of Soil, Plant and Food Science, University of Bari Aldo Moro, Via Amendola 165/A, 70126 Bari, Italy
simone.pascuzzi@uniba.it

[3] Institute of Technology, Estonian University of Life Sciences, 56 Kreutzwaldi Str., 51006 Tartu, EE, Estonia

[4] Polytechnic Institute of Bragança, Mountain Research Center, Bragança, Portugal

[5] Department Od Machine Operation and Production Processes Management, University of Life Sciences in Lublin, 13, Akademicka Str., 20-950 Lublin, Poland

[6] Dmytro Motornyi, Tavria State Agrotechnological University, 66 Zhukovsky Str., Zaporizhzhia 69600, UA, Ukraine

[7] Lublin University of Technology, Nadbystrzycka 38D, 20-618 Lublin, Poland

[8] PolySense Lab, Dipartimento Interateneo Di Fisica, Polytechnic and University of Bari, Via Amendola 173, 70126 Bari, Italy

[9] Polytechnic University of Bari, Via Edoardo Orabona 4, 70126 Bari, Italy

Abstract. The aim of the study is to enhance the operational characteristics of a screw conveyor during overloading of its working mechanism by substantiating the rational parameters of the safety coupling. Theoretical calculations and their graphical dependencies were performed using the Delphi programming environment. To increase the magnitude of axial displacement of the driven half-coupling with the jammed working element, while reducing dynamic loads during overloading, a design of a safety coupling has been developed. To determine the rational parameters of the safety coupling for the screw conveyor, the influence of dynamic loads on the operation of the safety coupling during overloading of the screw conveyor's working mechanism has been analyzed. From the analysis of the graphs, it has been determined that an increase in the rotation frequency n leads to an increase in the torque of the system. With a change in rotation frequency from 50 rpm to 200 rpm, the torque T_d increases by 64.8%, T_r rises by 65.2%, and T_m increases by 63.8%. It has also been determined that an increase in the mass m of moving links leads to an increase in loads on the drive. When the mass increases from 10 kg to 20 kg, the torque T_d increases by 15.8%, T_r rises by 12.5%, and T_m increases by 17.3%.

E. Lorencowicz et al. (Eds.): FMPMSA 2024, LNCE 609, pp. 87–97, 2024.
https://doi.org/10.1007/978-3-031-70955-5_10

Keywords: Safety Coupling · Half-Coupling · Groove · Rational Parameters · Dynamic Loading

1 Introduction

Technological processes in agricultural production involve many labor-intensive loading, unloading, and transportation operations [1–6]. Most commonly, these operations include the handling and transportation of grain crops, seed materials, granulated mineral fertilizers, and so on [7–10]. Screw auger conveyors, as a separate technical element of transportation mechanisms, have found widespread use in the layout schemes of machines for loading or moving bulk and lump materials due to their simple design, ease of maintenance, and the ability to load and unload materials at any point along the technological line [11–14]. During the transportation of such materials, due to the presence of clearances between the rotating surface of the screw and the inner surface of the guiding pipe, jamming of the screw working element is possible. To restore the functionality of the conveyor, it is necessary to disengage the jammed edge of the screw in the axial direction from contact with the material. Subsequently, after removing the overload, the drive elements should ensure the initial position of the screw working element for transporting the material to the unloading zone [15–18]. These issues can be addressed by axially disengaging the jammed screw working element using ball safety couplings with a profiled design of the recesses, both when disengaging and engaging, at the exit and entry points [19–21]. For the reliable operation of screw conveyors, both rigid [22] and flexible [23], specific designs of safety couplings have been developed for axial disengagement of a jammed screw, along with methodologies for conducting experimental research [24]. Considerable attention is given to analyzing the determination of dynamic loads in various types of drives with safety couplings, as well as their strength calculations [25–29]. Therefore, the task of developing new designs of safety couplings for screw conveyors to axially disengage the working element in case of overloading and ensure the restoration of its initial position is relevant. The aim of the research is to enhance the operational characteristics of the screw conveyor during overloading of its working mechanism by substantiating the rational parameters of the safety coupling.

2 Materials and Methods

To address this issue, a safety coupling with temporally separated slipping and axial displacement modes of the screw has been developed to restore the operational state of the screw conveyor. Its design and overall view are presented in Fig. 1. When transmitting torque, the cylindrical fingers (Fig. 1–4), which have a spherical shape on the working side and they are located in through axial openings in the anti-friction bushings (Fig. 1–5) of the driven half-coupling (Fig. 1–3), engage with the recesses (Fig. 1–7) of the driving half-coupling (Fig. 1–1). This ensures the rotation of the safety coupling and the screw working element (Fig. 1–3). The fingers (Fig. 1–4) and recesses (Fig. 1–7) are arranged at the same diameter, and on both sides of the recesses on the end surface

of the driving half-coupling (Fig. 1), there are circular working (Fig. 1–10) and return (Fig. 1–11) grooves. The inclination angle of the working groove is significantly smaller than the inclination angle of the return groove. In the event of an overload, the driven half-coupling (Fig. 1–3) stops while the driving half-coupling (Fig. 1–1) continues to rotate, causing the cylindrical fingers (Fig. 1–4) to disengage from the recesses (Fig. 1–7). During this process, the cylindrical fingers (Fig. 1–4) move along the circular working grooves (Fig. 1–10). Due to the rotation of the driving half-coupling (Fig. 1–1), the cylindrical fingers (Fig. 1–4) return to their initial position, resulting in the restoration of the initial state. During this process, the cylindrical fingers (Fig. 1–4) move along the circular return grooves (Fig. 1–11).

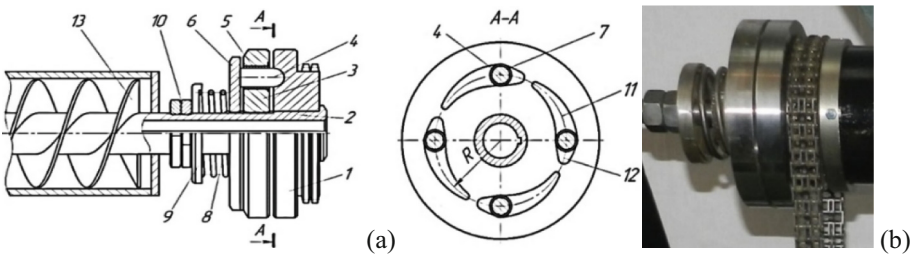

Fig. 1. Constructive diagram (a) and general view (b) of the safety coupling.

In determining the rational parameters of the screw conveyor's safety coupling, it is essential to consider the effect of dynamic loads, the absolute values of which will differ from static ones. To address this, a dynamic model of the screw conveyor with the safety coupling was examined, as shown in Fig. 2. It is described by a system of differential equations of motion (1):

$$\left.\begin{aligned} J_1 \cdot \ddot{\varphi}_1 &= T_d - c_1(\varphi_1 - \varphi_2), \\ J_{21} \cdot \ddot{\varphi}_2 &= c_1(\varphi_1 - \varphi_2) - T_m, \\ J_{22} \cdot \ddot{\varphi}_3 &= T_m - c_2(\varphi_3 - \varphi_4), \\ J_3 \cdot \ddot{\varphi}_4 &= c_2(\varphi_3 - \varphi_4) - T_r, \end{aligned}\right\} \tag{1}$$

where: c_1– equivalent torsional stiffness of the drive components between the engine and the driving half-coupling; c_2– equivalent torsional stiffness of the drive components between the driving half-coupling and the shaft of the working element; φ_1 – twist angle of the engine shaft; φ_2 – twist angle of the driving half-coupling; φ_3 – twist angle of the driven half-coupling; φ_4 – twist angle of the shaft of the working element; J_1 – consolidated moment of inertia of the drive; J_{21} – consolidated moment of inertia of the driving half-coupling; J_{22} – consolidated moment of inertia of the driven half-coupling; J_3– consolidated moment of inertia of the shaft of the working element; T_d – torque moment of the drive; T_m – torque moment of interaction between half-couplings; T_r – resistance moment on the shaft of the screw working element.

The drive torque moment T_d can be expressed as a constant moment:

$$T_d = T_{d0}, \tag{2}$$

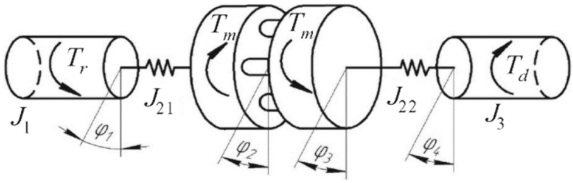

Fig. 2. Dynamic model of the screw conveyor with a safety coupling.

or as a linear characteristic of the electric drive in the form:

$$T_d = T_{d0}\left(1 - \frac{\dot{\varphi}_1}{\omega_0}\right), \tag{3}$$

where ω_0 is the angular velocity of rotation of all masses at the initial moment of time.

The resistance moment applied to the output link – the screw working element, T_r can be expressed as a constant moment:

$$T_r = T_{r0}, \tag{4}$$

or linearly increasing in the form:

$$T_r = T_{r0} + T_{r1} \cdot \frac{t}{\tau}. \tag{5}$$

Until the moment of time τ when complete stoppage of the screw occurs (its jamming).

The magnitude of the torque moment of interaction between half-couplings T_m is influenced by parameters such as the geometric dimensions of the half-coupling, the profiles of the recess and groove, the stiffness and initial tension of the compression spring, and the axial mass of the driven half-coupling together with the working element and a portion of the load. The influence of friction forces can be neglected since, with proper lubrication, it is sufficiently small.

Therefore, the moment T_m will be equal to the sum of two components – static, which depends on the deformation of the spring, and inertial, which is determined by the axial acceleration of the half-coupling.

The static component of the axial force during mutual displacement of half-couplings is equal to:

$$F_s = c(\delta_0 + \lambda), \tag{6}$$

where: δ_0 – initial tension of the spring; λ – current deformation of the spring, which is equal to the amount of the cylindrical finger exiting from recess; c – stiffness of the spring.

The dynamic component of the axial force was determined as the inertia force during the axial displacement of the driven half-coupling together with the working element and a portion of the load:

$$F_d = m\ddot{\lambda}, \tag{7}$$

where m is the mass of the driven links.

To determine the geometric relationships when the cylindrical finger exits from recess, a calculation scheme was constructed, as shown in Fig. 3.

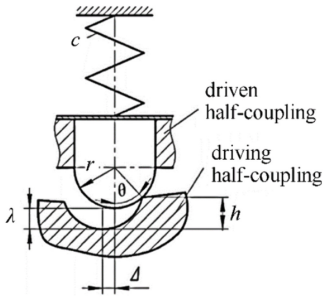

Fig. 3. Calculation scheme for determining the geometric relationships when the cylindrical finger exits from recess.

The tangential displacement of the cylindrical finger is equal to:

$$\Delta = R \cdot (\varphi - \varphi_3),$$

where R is the radius of the placement of the cylindrical fingers.

At the same time, the finger rises to a height λ, which is determined by the formula:

$$h - \lambda = r \cdot (1 - \cos\theta), \tag{8}$$

where: r is the radius of rounding of the cylindrical finger and θ is the current angle of the cylindrical finger pressing on the edge of the recess.

After substitutions and transformations, we obtain the expression:

$$\lambda = r \cdot (\cos\theta - \cos\theta_0), \tag{9}$$

where: θ_0 is the initial value of the angle of pressure of the cylindrical finger on the edge of the recess when the finger was completely in the recess.

The tangential displacement Δ of the cylindrical finger was determined through the angles of pressure:

$$\Delta = r \cdot (\sin\theta_0 - \sin\theta) = R \cdot (\varphi_2 - \varphi_3) = r \cdot (\sin\theta_0 - \sin\theta). \tag{10}$$

From Eqs. (9) and (10) we obtained:

$$\lambda = h - r + \sqrt{r^2 - [r \cdot \sin\theta_0 - R \cdot (\varphi_2 - \varphi_3)]^2}. \tag{11}$$

The current pressing angle of the finger is determined from (9) and (10), using (11), through the tangent of the angle θ:

$$\tan\theta = \frac{r \cdot \sin\theta_0 - R \cdot (\varphi_2 - \varphi_3)}{\lambda + r - h} = \frac{r \cdot \sin\theta_0 - R \cdot (\varphi_2 - \varphi_3)}{\sqrt{r^2 - [r \cdot \sin\theta_0 - R \cdot (\varphi_2 - \varphi_3)]^2}} \tag{12}$$

From here, the interaction torque of the half-couplings was determined by the equation:

$$T_m = R \cdot \tan\theta \cdot (F_s + F_d) = R\left[c(\lambda_0 + \lambda) + m_4 \cdot \ddot{\lambda}\right] \cdot \frac{r \cdot \sin\theta_0 - R \cdot (\varphi_2 - \varphi_3)}{\sqrt{r^2 - [r \cdot \sin\theta_0 - R \cdot (\varphi_2 - \varphi_3)]^2}} \tag{13}$$

By differentiating (11) with respect to time, the derivatives were determined $\dot{\lambda}$ and $\ddot{\lambda}$:

$$\begin{aligned}
\dot{\lambda} &= \frac{[r \cdot \sin\theta_0 - R(\varphi_2 - \varphi_3)] \cdot R \cdot (\dot{\varphi}_2 - \dot{\varphi}_3)}{\sqrt{r^2 - [r \cdot \sin\theta_0 - R \cdot (\varphi_2 - \varphi_3)]^2}}; \\
\ddot{\lambda} &= \frac{[r \cdot \sin\theta_0 - R(\varphi_2 - \varphi_3)] \cdot R(\ddot{\varphi}_2 - \ddot{\varphi}_3) - (R)^2 \cdot (\dot{\varphi}_2 - \dot{\varphi}_3)^2}{\sqrt{r^2 - [r \cdot \sin\theta_0 - R \cdot (\varphi_2 - \varphi_3)]^2}} \\
&- \frac{[r \cdot \sin\theta_0 - R \cdot (\varphi_2 - \varphi_3)]^2 \cdot (R)^2 \cdot (\dot{\varphi}_2 - \dot{\varphi}_3)^2}{\left(r^2 - [r \cdot \sin\theta_0 - R \cdot (\varphi_2 - \varphi_3)]^2\right)\sqrt{r^2 - [r \cdot \sin\theta_0 - R \cdot (\varphi_2 - \varphi_3)]^2}}.
\end{aligned} \tag{14}$$

Substituting Eqs. (11) and (14) into the expression for the interaction torque of the half-couplings (13), we get:

$$\begin{aligned}
T_m = &\left\{R\left[c\left(\delta_0 + h - r + \sqrt{r^2 - [r \cdot \sin\theta_0 - R(\varphi_2 - \varphi_3)]^2}\right)\right]\right. \\
&+ mR\left\{\frac{[r \cdot \sin\theta_0 - R \cdot (\varphi_2 - \varphi_3)]R \cdot (\ddot{\varphi}_2 - \ddot{\varphi}_3) - (R)^2 \cdot (\dot{\varphi}_2 - \dot{\varphi}_3)^2}{\sqrt{r^2 - [r \cdot \sin\theta_0 - R \cdot (\varphi_2 - \varphi_3)]^2}}\right. \\
&\left.\left. - \frac{[r \cdot \sin\theta_0 - R \cdot (\varphi_2 - \varphi_3)]^2 \cdot (R)^2 \cdot (\dot{\varphi}_2 - \dot{\varphi}_3)^2}{\left(r^2 - [r \cdot \sin\theta_0 - R \cdot (\varphi_2 - \varphi_3)]^2\right) \cdot \sqrt{r^2 - [r \cdot \sin\theta_0 - R \cdot (\varphi_2 - \varphi_3)]^2}}\right\}\right\} \\
&\times \frac{r \cdot \sin\theta_0 - R \cdot (\varphi_2 - \varphi_3)}{\sqrt{r^2 - [r \cdot \sin\theta_0 - R \cdot (\varphi_2 - \varphi_3)]^2}}.
\end{aligned} \tag{15}$$

The torque depends on the structural, mass, and elastic characteristics of the coupling, as well as the difference in the angles of mutual rotation of the half-couplings and their derivatives. Then, the initial conditions for the system motion were considered.

The most significant dynamic loads will occur in the case of a sudden jamming of the system, which is associated with the impact mechanism of the drive operation. In the case of a soft jamming, the process occurs more slowly, and dynamic loads will accordingly be less significant.

In the worst-case scenario, i.e., during a sudden jamming, the system transforms into a two-mass one, as the rotational mass J_3 comes to a halt, and the angle $\varphi_4 = 0$.

The deformation of the elastic links at the initial moment in time is determined by the torque of resistance T_r preceding the jamming time:

$$\begin{aligned}
&c_1(\varphi_{10} - \varphi_{20}) = T_r;\ c_1(\varphi_{30} - \varphi_{40}) = T_r; \\
&\varphi_{20} = \varphi_{30};\ \varphi_{40} = 0.
\end{aligned} \tag{16}$$

The third equation shows that the coupling rotates as a single unit.

Here, the subscript "0" denotes the initial value when the cylindrical finger was fully in the recess. The rotational velocities of all masses at the initial moment were the same and equal to ω_0.

$$\dot{\varphi}_{10} = \omega_0; \dot{\varphi}_{20} = \omega_0; \dot{\varphi}_{30} = \omega_0; \dot{\varphi}_{40} = 0. \tag{17}$$

So, Eqs. (1) and (15), along with the characteristics of the drive (2) or (3) and resistance (4) or (5), initial conditions (16) and (17), constitute the mathematical model of the motion of the screw conveyor's safety clutch system. The system is too complex for analytical solution, so numerical integration methods based on the well-known Runge-Kutta technique were applied.

To transform the system of second-order differential equations into a system of first-order differential equations, the following variable substitution was performed:

$$u = \dot{\varphi}_1; v = \dot{\varphi}_2; w = \dot{\varphi}_3. \tag{18}$$

Accordingly, after differentiating (18), we obtain:

$$\dot{u} = \ddot{\varphi}_1; \dot{v} = \ddot{\varphi}_2; \dot{w} = \ddot{\varphi}_3. \tag{19}$$

The expression for the interaction torque T_m contains the values of second derivatives of angles, which complicates the application of the numerical method. After substitutions and appropriate transformations, we obtain the final formula for determining the interaction torque T_m in the form:

$$T_m = \frac{m \cdot R^2\left(r^2 - k\right)\left[\frac{c_1(\varphi_2-\varphi_3)}{J_{21}} + \frac{c_2(\varphi_2-\varphi_3)}{J_{22}}\right] + m \cdot R^3 \cdot (\dot{\varphi}_2 - \dot{\varphi}_3)^2 \cdot \sqrt{r^2 - k}}{k + m \cdot R^2 \cdot \left(r^2 - k\right) \cdot \frac{J_{21}+J_{22}}{J_{21} \cdot J_{22}}} + \frac{mR^3 \cdot (\dot{\varphi}_2 - \dot{\varphi}_3) \cdot \sqrt{\left(r^2 - k\right)^3} + c \cdot R\left(\lambda_0 + h - r + \sqrt{k}\right) \cdot \sqrt{k^3 \cdot \left(r^2 - k\right)}}{k\left[k + m \cdot R^2 \cdot \left(r^2 - k\right) \cdot \frac{J_{21}+J_{22}}{J_{21} \cdot J_{22}}\right]}, \tag{20}$$

where $k = r^2 - [r \cdot \sin\theta_0 - R(\varphi_2 - \varphi_3)]^2$.

Using the substitutions and replacements mentioned above, we obtain the final system of first-order differential equations:

$$\begin{aligned} &\dot{u} = \frac{T_d - c_1(\varphi_1 - \varphi_2)}{J_1}; \dot{v} = \frac{c_1(\varphi_1 - \varphi_2) - T_m}{J_{21}}; \\ &\dot{w} = \frac{T_m - c_2(\varphi_3 - \varphi_4)}{J_{22}}; \dot{\varphi}_1 = u; \dot{\varphi}_2 = v; \dot{\varphi}_3 = w. \end{aligned} \tag{21}$$

Initial conditions, considering the transformations and substitutions, will take the form:

$$\varphi_{10} = \frac{T_r}{c_1} + \frac{T_r}{c_2}; \varphi_{20} = \frac{T_r}{c_2}; \varphi_{30} = \frac{T_r}{c_2}; u_0 = \omega_0; v_0 = \omega_0; w_0 = \omega_0. \tag{22}$$

3 Results and Discussions

Theoretical calculations of the obtained analytical dependencies and their graphical interpretation were performed on a PC using the Delphi programming environment.

To implement the numerical solution of the mathematical model described by Eqs. (20)–(22), a program was developed in the Pascal language within the Delphi visual programming environment. This program allows for the construction of graphical dependencies and the investigation of the influence of various system parameters on dynamic loads in the drive links of the screw conveyor.

The graphic dependencies illustrating the change in the torque magnitude during the slipping of the half-coupling are presented in Fig. 4.

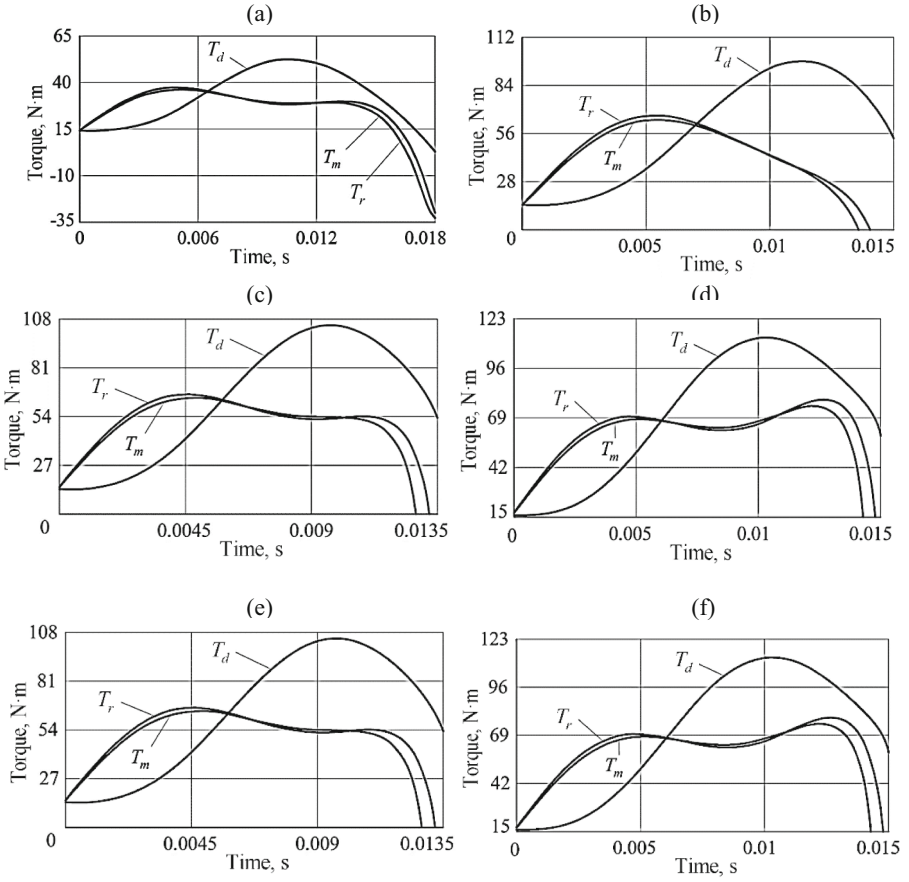

Fig. 4. Time-dependent plots of the torque moments T_d, T_r and T_m during the slip of the half-couplings: (a) – $m = 10$ kg, $n = 50$ rpm; (b) – $m = 10$ kg, $n = 100$ rpm; (c) – $m = 10$ kg, $n = 150$ rpm; (d) – $m = 10$ kg, $n = 200$ rpm; (e) – $m = 15$ kg, $n = 100$ rpm; (f) – $m = 20$ kg, $n = 100$ rpm.

The drive torque is equal to $T_d = c_1(\varphi_2 - \varphi_1)$, and the moment arising in the jammed driven half-coupling and screw working element is equal to $T_r = c_2\varphi_3$. In the numerical calculations, the following parameter values were adopted: $J_1 = 40\,\text{kg}\cdot\text{m}^2$; $J_{21} = 0.0157\,\text{kg}\cdot\text{m}^2$; $J_{22} = 0.00925\,\text{kg}\cdot\text{m}^2$; $c_1 = c_2 = 1600\,\text{N}\cdot\text{m}\cdot\text{rad}^{-1}$; $c = 10000\,\text{N}\cdot\text{m}^{-1}$; $h = 4.6$ mm; $r = 12$ mm; $R = 60$ mm; $\delta_0 = 20$ mm. In this case, the rotation frequency n varied within the range of 50 to 200 revolutions per minute, and the mass of the driven links m ranged from 10 kg to 20 kg. Based on the conducted dynamic analysis of the safety coupling operation in the screw conveyor, it has been determined that an increase in the rotation frequency of the working mechanism leads to an increase in the torque moments of the system.

The graphs show that when the moment T_r arising in the jammed screw working element reaches the permissible drive moment T_d, i.e., the moment of interaction of the half-couplings T_m (the moment of the safety clutch operation provided by its design parameters), the smooth axial deflection of the screw occurs, returning it to its previous position. In this process, the cause of the working element jamming is eliminated, reducing the torque moments of the system, and the initial state is restored.

From the analysis of the graphs (Fig. 4, a-d), it has been determined that with a change in rotation frequency from 50 rpm to 200 rpm, the torque T_d increases by 64.8%, T_r rises by 65.2%, and T_m increases by 63.8%. Also, from the graphs (Fig. 4b, d, e), it has been established that an increase in mass m of moving links leads to an increase in loads on the drive. When the mass increases from 10 kg to 20 kg, the torque moment T_d increases by 15.8%, T_r rises by 12.5%, and T_m increases by 17.3%.

The obtained mathematical model allows determining the influence of key parameters on the dynamics of the safety coupling operation in the screw conveyor during overloading of the working mechanism. Thus, by applying the provided mathematical model, it is possible to select rational design and kinematic parameters for the developed safety coupling of the screw conveyor with respect to its engagement moment.

Subsequently, it is advisable to conduct research to determine the magnitude of contact stresses in the engagement elements during the operation of the safety coupling. This will enable the selection of material for the half-coupling of the safety coupling in the screw conveyor, ensuring strength conditions under contact stresses. The level of these stresses is a crucial factor influencing the wear intensity of contact surfaces.

4 Conclusions

Based on the dynamic model of the screw conveyor with the safety coupling, differential equations of motion for the system elements have been formulated.

Theoretical investigations have resulted in the construction of graphical dependencies illustrating changes in the torque magnitude during the slipping of the half-coupling of the safety coupling. These graphs serve to explore the influence of various system parameters on the dynamic loads in the drive links of the screw conveyor. From the analysis of the graphs, it has been determined that an increase in the rotation frequency n leads to an increase in the torque of the system.

With a change in rotation frequency from 50 rpm to 200 rpm, the torque T_d increases by 64.8%, T_r rises by 65.2%, and T_m increases by 63.8%. Also, from the graphs (Fig. 4b,

d, e), it has been established that an increase in mass m of moving links leads to an increase in loads on the drive. When the mass increases from 10 kg to 20 kg, the torque moment T_d increases by 15.8%, T_r rises by 12.5%, and T_m increases by 17.3%.

Based on the conducted dynamic analysis of the safety coupling operation in the screw conveyor, it has been determined that an increase in the rotation frequency of the working mechanism leads to an increase in the torque within the system.

References

1. Bulgakov, V., Pascuzzi, S., Nadykto, V., Ivanovs, S., Adamchuk, V.: Experimental study of the implement-and-tractor aggregate used for laying tracks of permanent traffic lanes inside controlled traffic farming systems. Soil Tillage Res. **208**, 104895 (2021)
2. Bulgakov, V., Pascuzzi, S., Ivanovs, S., Nadykto, V., Nowak, J.: Kinematic discrepancy between driving wheels evaluated for a modular traction device. Biosys. Eng. **196**, 88–96 (2020)
3. Pascuzzi, S., Anifantis, A.S., Santoro, F.: The concept of a compact profile agricultural tractor suitable for use on specialised tree crops. Agriculture **10**, 123 (2020)
4. Bulgakov, V., Pascuzzi, S., Beloev, H., Ivanovs, S.: Theoretical investigations of the headland turning agility of a trailed asymmetric implement-and-tractor aggregate. Agriculture **9**, 224 (2019)
5. Bulgakov, V., Pascuzzi, S., Anifantis, A.S., Santoro, F.: Oscillations analysis of front-mounted beet topper machine for biomass harvesting. Energies **12**, 2774 (2019)
6. Bulgakov, V., Pascuzzi, S., Adamchuk, V., Kuvachov, V., Nozdrovicky, L.: Theoretical study of transverse offsets of wide span tractor working implements and their influence on damage to row crops. Agriculture **9**, 144 (2019)
7. Pascuzzi, S., Santoro, F., Manetto, G., Cerruto, E.: Study of the correlation between foliar and patternator deposits in a "Tendone" vineyard. Agric. Eng. Int. CIGR J. **20**(3), 97–107 (2018)
8. Pascuzzi, S., Blanco, I., Anifantis, A.S., Scarascia Mugnozza, G.: Electrolyzer performance analysis of an integrated hydrogen power system for greenhouse heating. A Case Study. Sustain. **8**, 629 (2016)
9. Pascuzzi, S.: Outcomes on the spray profiles produced by the feasible adjustments of commonly used sprayers in "Tendone" vineyards of Apulia (Southern Italy). Sustainability **8**(12), 1307 (2016)
10. Pascuzzi, S., Cerruto, E.: An innovative pneumatic electrostatic sprayer useful for tendone vineyards. J. Agric. Eng. **458**, 123–127 (2015)
11. Hevko, R.B., Klendiy, O.M.: The investigation of the process of a screw conveyer safety device actuation. INMATEH Agric. Eng. **42**(1), 55–60 (2014)
12. Pascuzzi, S., et al.: Theoretical study of the motion of a cut sugar beet tops particle along the inner surface of the conveying and unloading system of a topping machine. Agric. Eng. **6**, 409–422 (2024)
13. Hevko, R.B., Rozum, R.I., Klendiy, O.M.: Development of design and investigation of operation processes of loading pipes of screw conveyors. INMATEH Agric. Eng. **50**(3), 89–96 (2016)
14. Pascuzzi, S., Łyp-Wrońska, K., Gdowska, K., Paciolla, F.: Sustainability evaluation of hybrid agriculture-tractor powertrains. Sustainability **16**(3), 1184 (2024)
15. Hevko, R.B., Klendiy, M.B., Klendiy, O.M.: Investigation of a transfer branch of a flexible screw conveyer. INMATEH Agric. Eng. **48**(1), 29–34 (2016)
16. Kováčová, M., Matus, M., Krizan, P., Beniak, J.: Design theory for the pressing chamber in the solid biofuel production process. Acta Polytechnica **54**(1), 28–34 (2014)

17. Güneş, E.C., Çelik, I.: Use of disc springs in a pellet fuel machine. Czech Techn. Univ. Prague Acta Polyt.s **57**(2), 89–96 (2017)
18. Bulgakov, V., et al.: Justification of parameters for novel rotary potato harvesting machine. Agron. Res. **19**(2), 984–1007 (2021)
19. Trokhaniak, O.M., Hevko, R.B., Lyashuk, O.L., Dovbush, TA, Pohrishchuk, B.V., Dobizha, N.V.: Research of the of bulk material movement process in the inactive zone between screw sections. INMATEH Agric. Eng. **60**(1), 261–268 (2020)
20. Bulgakov, V., Holovach, I., Ruzhylo, Z., Fedosiy, I., Ihnatiev, Y., Olt, J.: Theory of oscillations performed by tools in spiral potato separator. Agron. Res. **18**(1), 38–52 (2020)
21. Adamchuk, V., Bulgakov, V., Ivanovs, S., Holovach, I., Ihnatiev, Y.: Theoretical study of pneumatic separation of grain mixtures in vortex flow. Eng. Rural Devel. **20**, 657–664 (2021)
22. Sokil, B., Lyashuk, O., Sokil, M., Popovich, P., Vovk, Y., Perenchuk, O.: Dynamic effect of cushion part of wheeled vehicles on their steerability. Int. J. Autom. Mech. Eng. **15**(1), 4880–4892 (2018)
23. Aulin, V.V., Pankov, A.O., Zamota, T.M., Lyashuk, O.L., Hrynkiv, A.V., Tykhyi, A.A., Kuzyk, A.V.: Development of mechatronic module for the seeding control system. Inmateh Agric. Eng. **59**(3), 1–8 (2019)
24. Lyashuk, O., Vovk, Y., Sokil, B., Klendii, V., Ivasechko, R., Dovbush, T.: Mathematical model of a dynamic process of transporting a bulk material by means of a tube scraping. Agric. Eng. Int. CIGR J. **21**(1), 74–81 (2019)
25. Gevko, R.B., Klendiy, O.M.: The investigation of the process of a screw conveyer safety device actuation INMATEH. Agric. Eng. **42**(1), 55–60 (2014)
26. Annunziato, A., Godfrey, M., Anelli, F., Dulieu-Barton, J., Holmes, C., Prudenzano, F.: Flexible photonic sensors: investigation of an approach based on ratiometric power in few-mode waveguides for bending measurement. IEEE Access (2024)
27. Merritt, A.S., Mair, R.J.: No access mechanics of tunnelling machine screw conveyors: model tests. Géotechnique **56**(9), 605–615 (2015)
28. Anelli, F., Annunziato, A., Erario, A., Holmes, C., Ciminelli, C., Prudenzano, F.: Design of microstructured flat optical fiber for multiaxial strain monitoring in composite materials. J. Lightwave Technol. **40**(17), 5986–5994 (2022)
29. Paul, Ph.J., Cleary, W.: Screw conveyor performance: comparison of discrete element modelling with laboratory experiments. Progr. Computat. Fluid Dyn. Int. J. **10**, 5–6 (2010)

Author Index

E. Lorencowicz et al. (Eds.): FMPMSA 2024, LNCE 609, pp. 497–499, 2024.
https://doi.org/10.1007/978-3-031-70955-5